

How well do discrete element granular flow models capture the essentials of mixing processes?

Paul W. Cleary¹, Guy Metcalfe² and Kurt Liffman²

¹ CSIRO Division of Mathematical and Information Sciences, Clayton, Victoria.

² CSIRO Division of Building, Construction and Engineering, Highett, Victoria.

ABSTRACT

Flowing granular materials, undergoing both mixing and segregation, play important roles in industries ranging from minerals and food to pharmaceuticals and ceramics. Sometimes it is desirable to enhance the mixing and inhibit segregation and in other cases it is desirable to minimise the mixing and enhance the segregation. The fundamentals of these processes are poorly understood. Computational modelling of such granular flows offers an good opportunity to study these fundamentals. But how well do these discrete element based modelling techniques capture the essential features of mixing processes?

The capabilities of our discrete element modelling package are described. Two different methods for measuring the rates of mixing are presented and three different configurations are studied. Qualitatively reasonable flows are obtained. A detailed study of the mixing demonstrates that the amount and nature of the mixing is quite sensitive to a range of physical parameters.

1. NOMENCLATURE

A - mean value of distribution a_i
 h - fill level of the tumbler: range $[0,1]$
 m_i - weighting of i th value in distribution
 $M = \sum_i m_i$ N - number of particles
 n_a - ave number of particles in a local average
 R - tumbler radius = 15 cm
 ϵ - Coefficient of restitution
 η - coefficient of variation ω - rotation rate
 μ - Surface friction σ - standard deviation

2. OVERVIEW OF PACKAGE

CSIRO's Division of Mathematical and Information Sciences has developed a two dimensional package based on a discrete ele-

ment method. It consists of a graphical pre-processor that is used to construct the problem geometry, a main simulation code and a range of post-processing programs that are used to analyse the flows.

Boundary objects of nearly arbitrary shape are constructed from line, circular or disc primitives. Flows in the complex geometries found in industrial applications can then be modelled. Rigid body and surface motions can be specified and external forces can be attached. The particles are modelled as discs. Packed particle microstructures are built by filling user specified polygons with particles having any size and density distributions.

The main code uses the pre-processor and other information to perform the required simulation. The flows can then be analysed with an array of visualisation and data processing tools to provide information such as wear rates and distributions, collision forces, dynamic loads on boundaries, sampling and flow statistics, mixing and segregation rates.

3. THE SIMULATION METHOD

The modelling technique is a soft particle method. The particles are allowed to overlap and the amount of overlap Δx , and the normal and tangential relative velocities determine the collisional forces. Figure 1 illustrates the collisional forces. The normal force F_n has a spring to provide the repulsive force that pushes the particles apart and a dashpot that provides dissipation, resulting in an effective coefficient of restitution. The tangential component has an incrementing spring and dashpot that is subject to the frictional limit.

The algorithm can be briefly summarised as having three key parts:

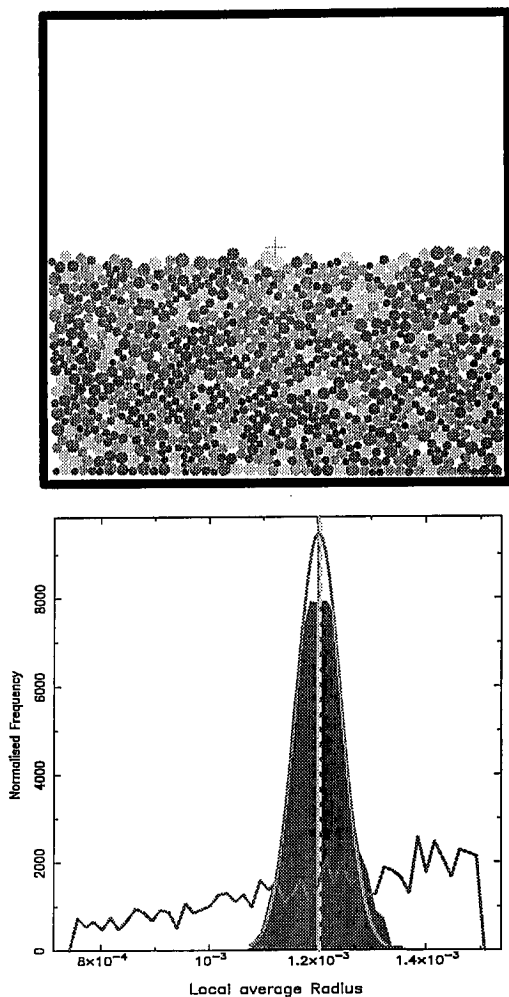


Figure 2: a) Random mixture of particles b) Distribution of local average particle radius.

what jagged and almost horizontal line. The vertical light grey line at 1.25 mm is the mean particle size. The light grey bell shaped curve is the predicted distribution of local average radius for the randomly mixed case. The dark shaded area is the actual local average distribution calculated. Note that this distribution is very close to that of the randomly mixed case. Its peak is a little shorter and its right edge extends slightly beyond that of the randomly mixed curve. This shows that the local average approach can identify mixtures that are very close to the theoretically randomly mixed case. Here the difference is only 3%.

Figure 3 shows fully segregated particles lying in four distinct layers. a) shows the particle layers and b) shows the relevant distributions. The light grey dashed vertical line is the mean radius. The light grey bell curve is the randomly mixed limit. The fully segregated limit is the mid grey line with four sepa-

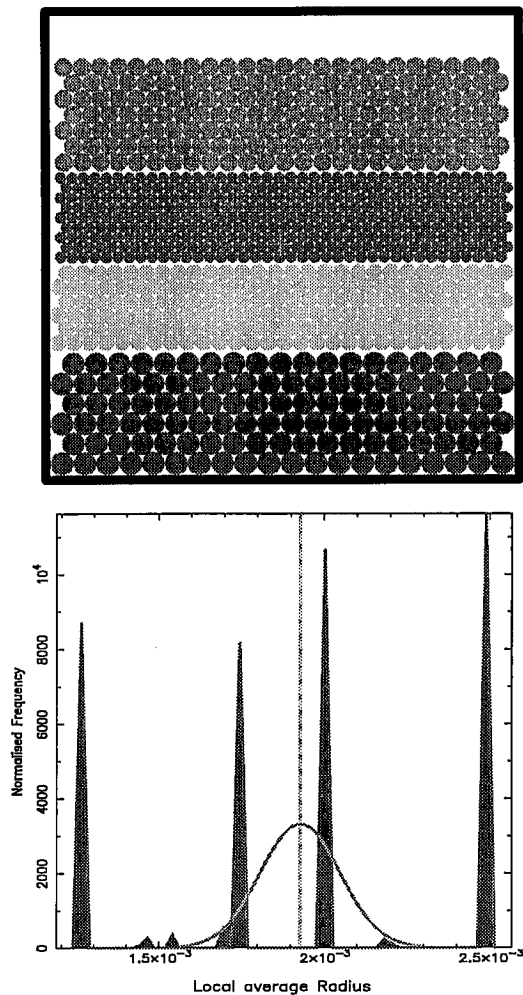


Figure 3: a) Four fully segregated layers b) Distribution of local average particle radius.

rate peaks, one for each of the layers. The actual local average distribution is the dark grey shaded area. This is almost indistinguishable from the curve delimiting the fully segregated limit. Note that there are three very small peaks between the main ones. This is the full extent of the aliasing produced by the local averages for the boxes that contain two different sizes of particles. $\xi = 0.97$ is only 3% from the fully segregated limit.

This technique is able to identify both the fully segregated and randomly mixed limits with high accuracy. It produces little aliasing of real peaks if the averaging box is chosen properly. It is a sensitive tool for analysing subtle variations in the mixing states.

5. MIXING IN A ROTATING BOX

We use the above method to analyse the changing state the mixture shown in Figure 3a when the box spins about its center at 15

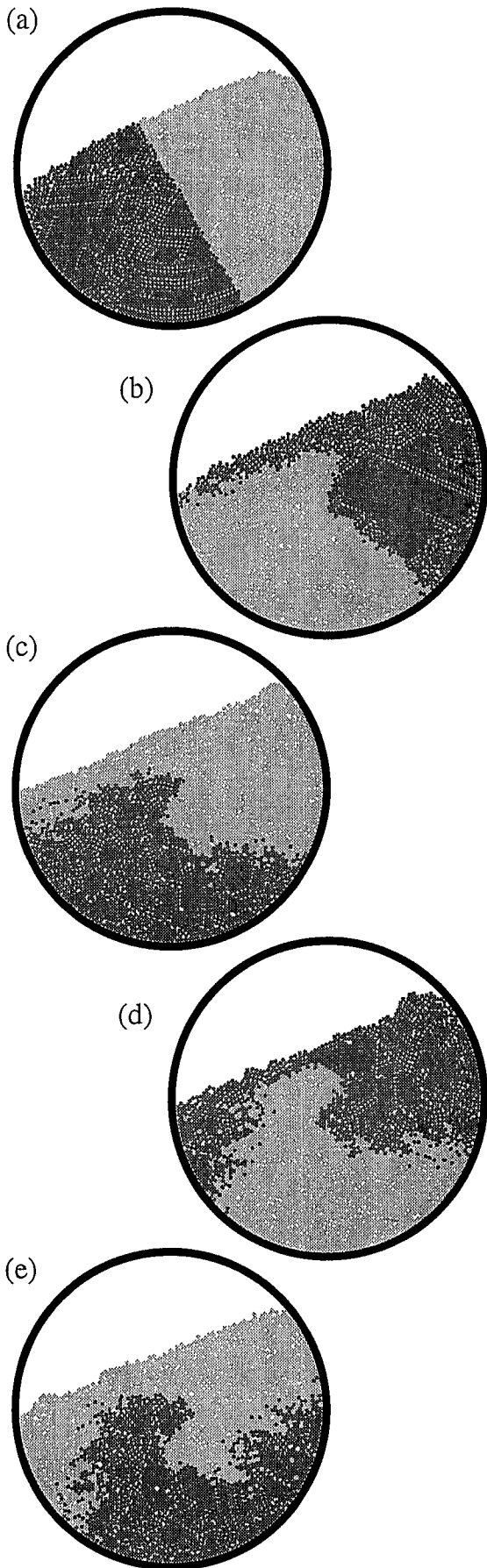


Figure 6: Mixing in a 60% loaded tumbler, a) $t = 2$ s, b) $t = 12$ s, c) $t = 22$ s, d) $t = 32$ s and e) $t = 42$ s

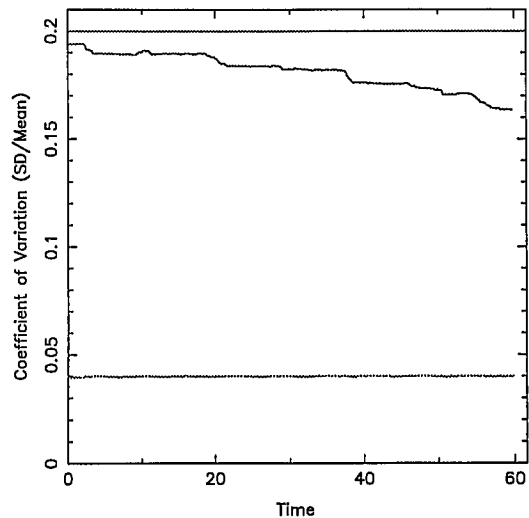


Figure 7: Mixing in a 60% loaded tumbler.

$\mu = 0.75$. This approximately matches the experimental setup of Metcalfe *et. al.* (1995).

Figure 6 shows snapshots of the flow. The particles are shaded (coloured) differently on the two sides of the tumbler in order to track the mixing. Frame a) shows the particles rotating as a rigid mass. This is demonstrated by the undeformed surface of the material and the line separating the two colours. At around $t = 3$ the angle of the surface exceeds the angle of failure and the material above this begins to avalanche. The particle motion is relatively simple: they rotate as a rigid mass until above the angle of failure and flow down the slope as a series of discrete avalanches. The demarcation between the two sets of particles is unchanged by any avalanches that consist of only one colour. If the boundary between the two regions passes through the thin avalanching layer or intersects the top surface then particles of both colours are able to mix.

The depth of the cascading layer is around 6 to 7 particles. This is consistent with the experiments. For fill levels higher than $h = 0.5$ or a 50% loading the particles near the center never participate in the surface avalanching. This is observed experimentally to lead to a precessing core of unmixed material. This can be also be clearly seen developing in the simulations. Figure 6b shows the configuration after light grey (red) material has flowed once over the surface of the dark grey (blue) material which is in turn just flowing back down over the light grey (red) material. The interface between the two materials has become

9. MIXING RATES

A series of simulations was performed to identify the effects of various physical parameters on the mixing. The base conditions were $\omega = 6$ rpm, $\mu = 1.0$, $\epsilon = 0.5$, particle mean size of 1.8 mm and a size variation of $\pm 2.4\%$.

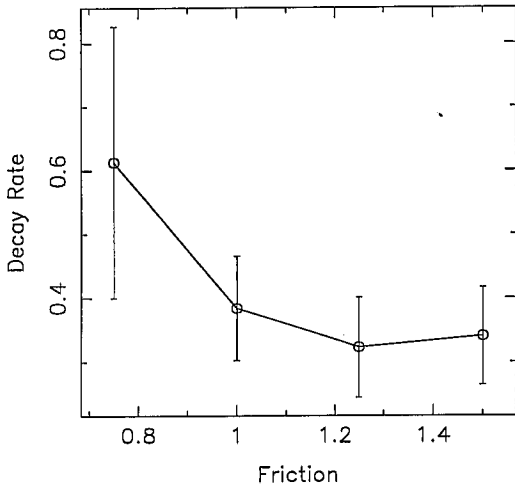


Figure 10: Variation of γ with μ .

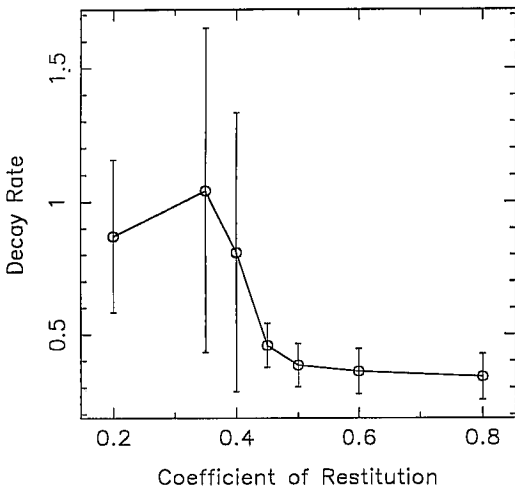


Figure 11: Variation of γ with ϵ .

Figures 10-12 show the behaviour of γ with changes in μ , ϵ and the size distribution. Both γ and T are relatively constant for $\mu \geq 1$ and both increase for lower values. This is caused by the flow developing a partially slumping and partially circulating motion. This speeds the mixing but slows the centroid exchange. There is a surprising sensitivity to ϵ . For $\epsilon \geq 0.5$, both γ and T are relatively constant. For lower values (increasingly dissipative flows) both γ and T increase sharply. There is also an abrupt increase in the error ranges. For very low ϵ the flows develop a hump towards the bottom of the down slope

as the avalanches have insufficient energy to reach the bottom of the tumbler in one movement. This seems to be connected to the increase in T . The mixing is relatively insensitive to small size variations in the particle sizes (Figures 12). Once the size variation reaches $\pm 20\%$ of the mean size, it begins to strongly affect the mixing rate which nearly doubles. The mixing period T steadily declines as the size variation increases.

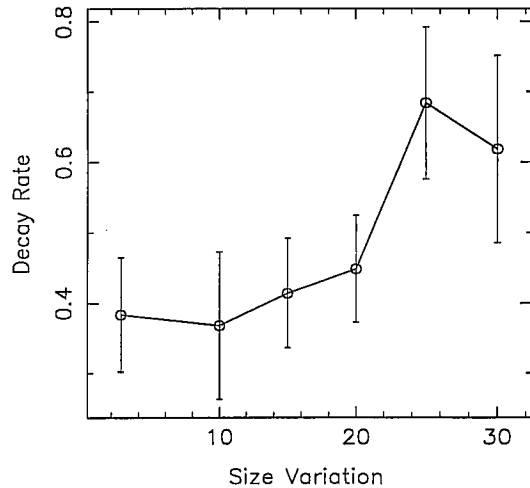


Figure 12: Variation with particle size range.

Further tests indicate that values of rolling friction as high as 0.025 g have no effect. This indicates that the frictional connection between the particles and the tumbler are already sufficient to prevent any sliding along the tumbler wall. A lower dynamic friction coefficient than the static one slightly increases both γ and T . Conversely, the rotation rate has a significant effect on the mixing rate by changing the flow regime. A slower rotation rate of 2.4 rpm gives γ about 35-65% larger than those for 6 rpm.

To check the numerical accuracy, four times the spring stiffness was used. This reduces the particle overlaps by a factor of four and is roughly the equivalent of mesh refinement for discrete element methods. There was no change in mixing rate or period.

10. EXPERIMENT COMPARISON

The experimental results for $h = 0.2$ gave $\gamma \approx 2.5$ and $T \approx 0.23$. These were obtained for cubic salt particles with a mean size of 1.01 mm, a size range of $\pm 20\%$ and a tumbler rotation of 2.5 rpm. The values of μ and ϵ are unknown. Our simulation overturning period